Cómo citar este artículo: I. F. Betancourt-Montañez, et al, "Evaluation of the structural, morphological magnetic properties of the $Bi_{1-x}SmxFeO_3$" Revista Ingeniería, Investigación y Desarrollo, vol. 22 (2), pp. 64-70, julio. 2022.

DOI: https://doi.org/10.19053/1900771X.v22.n2.2022.15024

EVALUATION OF THE STRUCTURAL, MORPHOLOGICAL MAGNETIC PROPERTIES OF THE $Bi_{1-X}Sm_XFeO_3$ SYSTEM

Evaluación de las propiedades estructurales, morfológicas y magnéticas del sistema $Bi_{1-x}SmxFeO_3$

Iván Fernando Betancourt Montañez[1], Christian Fabián Varela Olivera [2], Julián A. Munevar Cagigas[3], Santiago Sandoval Gutiérrez[4], César Armando Ortíz Otálora[5], Carlos A. Parra Vargas[6], Claudia Liliana Sánchez Sáenz[7]

[1-2-6] Grupo GFM, Facultad de Ciencias, Universidad Pedagógica y Tecnológica de Colombia, Tunja, Boyacá, Colombia. [1-4]Grupo de Sistemas Dinámicos, Universidad de los Llanos, km 12 Vía a Puerto López, Villavicencio, Meta Villavicencio, Colombia. [3]CCNH, Universidade Federal do ABC (UFABC), Santo André, SP 09210-580, Brasil. [5]Grupo GSEC, Facultad de Ciencias, Universidad Pedagógica y Tecnológica de Colombia, Tunja, Boyacá, Colombia. [7]Grupo de Investigación en Telemática y TIC aplicada a la Educación, Universidad Pedagógica y Tecnológica de Colombia, Tunja, Boyacá, Colombia. Email: [1]ivanbetancourt5@gmail.com, [2]christian.varela@uptc.edu.co, [3]julian.munevar@ufabc.edu.br, [4]ssandoval@unillanos.edu.co, [5]cesar.ortiz@uptc.edu.co, [6]carlos.parra@uptc.edu.co, [7]claudialiliana.sanchez1@uptc.edu.co

(Recibido 01 de julio de 2022 y aceptado 05 de agosto de 2022)

Resumen

Este artículo reporta la síntesis del sistema $Bi_{1-x}Sm_xFeO_3$ (x = 0.00, 0.02, 0.04, 0.06, 0.08 y 0.10) obtenido por el método de reacción en estado sólido a 1073.15 K durante 15 h. La caracterización permitió evaluar el efecto de la inserción de Sm^{3+} sobre las propiedades estructurales, morfológicas y magnéticas de la ferrita de bismuto. La caracterización estructural se realizó mediante Difracción de Rayos X (XRD) y refinamiento de Rietveld, lo que indica la formación de una fase romboédrica mayoritaria del grupo espacial R3c (161) con una proporción superior a la reportada hasta ahora. La caracterización morfológica mediante microscopía electrónica de barrido (SEM) permitió concluir que la inserción de samario disminuye el tamaño de partícula de 7.5 µm a 2.5 µm, gracias al menor radio iónico, que también condujo a la contracción de los parámetros reticulares. El análisis magnético mostró un comportamiento ferromagnético típico en todas las muestras sintetizadas, con la presencia de una transición PM-AFM a 260 K.

***Palabras clave*:** *estado sólido, ferrita de bismuto, samario, dopaje.*

Abstract

This paper reports the synthesis of the $Bi_{1-x}SmxFeO_3$ system (x = 0.00, 0.02, 0.04, 0.06, 0.08 and 0.10) obtained by the solid-state reaction method at 1073.15 K for 15 h. Characterization allowed evaluating the effect of Sm^{3+} insertion on the structural, morphological and magnetic properties of the bismuth ferrite. Structural characterization was made by X-ray Diffraction (XRD) and Rietveld refinement, indicating the formation of a rhombohedral majority phase of the space group R3c (161) with a proportion higher than the reported up to now. The morphological characterization through scanning electron microscopy (SEM) allowed concluding that the insertion of samarium decreases the particle size from 7.5 µm to 2.5 µm, thanks to the smaller ionic radius, which also led to the contraction of the lattice parameters. The magnetic analysis showed a typical ferromagnetic behaviour in all of the synthesized samples, with the presence of a PM-AFM transition at 260 K.

Key words: *solid-state, bismuth ferrite, samarium, doping.*

1. INTRODUCTION

Bismuth ferrite ($BiFeO_3$) is a multiferroic material that exhibits multiferroic properties dependent on its electrical polarization, magnetization, and elasticity. Among the properties are ferroelectricity, ferromagnetism, ferroelasticity at room temperature, high Curie and Neel temperature (T_C ~ 1103K, T_N ~ 643K) [1]. $BiFeO_3$-type materials are distorted perovskites with a rhombohedral space group R3c (167) [2]. Moreover, they are antiferromagnetic at room temperature and are arranged with a G-type spin configuration along the (1 1 1) or (0 0 1) direction in the rhombohedral structure.

Despite its relevant properties, $BiFeO_3$-type materials present secondary crystalline phases due to the Bi/Fe imbalance or loss of Bi [3]. Doping with rare earth elements from the lanthanide group in $BiFeO_3$ leads to structural distortions, which can improve the ferromagnetic or ferroelectric properties. This allows for technological applications such as: magnetic sensors, energy conversion, devices used in spintronics, magnetoelectric random access memories (MERAM) and other types of sensors [4].

In this work, the $Bi_{1-x}Sm_xFeO_3$ system (0.00, 0.02, 0.04, 0.06, 0.08 and 0.10) was produced by the solid-state reaction method and then characterized, in order to study the effect of samarium doping on the morphological, structural and magnetic properties.

2. EXPERIMENTAL CONDITIONS

All of the materials were prepared through the solid-state reaction method, using the following precursors: Bi_2O_3 (99.999%), Sm_2O_3 (99.99%) y del Fe_2O_3 (98.9%). Stoichiometric mixtures according to chemical formula $Bi_{1-x}Sm_xFeO_3$ with x = 0, 0.02, 0.04, 0.06, 0.08 and 0.1 were ground for 2 hours, pressed into pellets under axial pressure of 5.0 MPa and sintered at 1063.15 K for 15 hours.

Structural analysis was performed by X-ray Diffraction using a Panalytical X'Pert Pro equipment, with CuKα radiation (λ = 1.5406 Å), and a scanning step of 2.0° in the 2θ range 20 - 80°. GSAS [5] and PCW [6] software suites were used to make a structural refinement by the Rietveld method, and VESTA [7] software package allowed the 3D representation of the unit cell.

Morphological study of the samples was carried out by Scanning Electron Microscopy (SEM) at 2000x, using a JEOL JSM 6490-LV equipment at 20 kV. Finally, magnetic analysis of the samples was made with a vibrating sample magnetometer VersaLab model from Quantum Design, measurements were made as a function of the applied field at room temperature with a field range between 30 kOe and -30 kOe, and magnetization as a function of temperature (from 2 to 340 K) at constant fields of 5000 kOe.

3. RESULTS AND DISCUSSION

Obtained diffractograms for the $Bi_{1-x}Sm_xFeO_3$ system are shown in Fig. 1. Samples were labelled as a function of the value of x as BFO, BFO2, BFO3, BFO4, BFO6, BFO8 and BFO10 for 0.00, 0.02, 0.04, 0.06, 0.08 and 0.10, respectively. Except for the BFO sample, the others exhibited a predominant crystal phase corresponding to bismuth ferrite ($BiFeO_3$, JCPDS 01-073-0548) with a rhombohedral structure of space group R3c (161), and a secondary crystal phase corresponding to $Bi_2Fe_4O_9$ with orthorhombic structure of space group Pbam (55). Formation of secondary crystal phase can be attributed to low thermal stability of $BiFeO_3$ crystal phase, and bismuth volatilization [8].

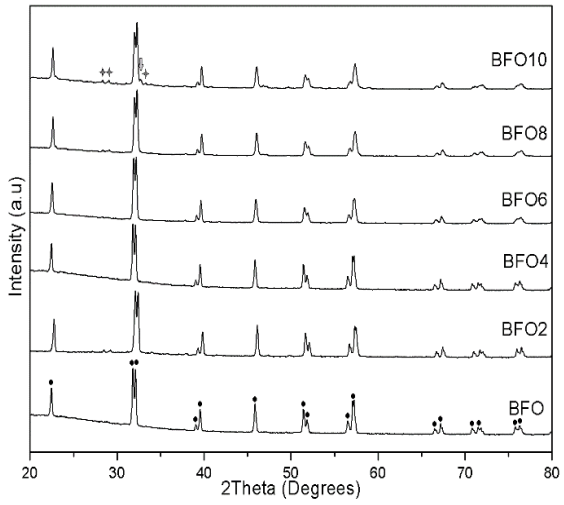

Figure 1. X-ray diffractograms of the $Bi_{1-x}Sm_xFeO_3$ samples: • main phase ($BiFeO_3$), • $Bi_2Fe_4O_9$ phase.

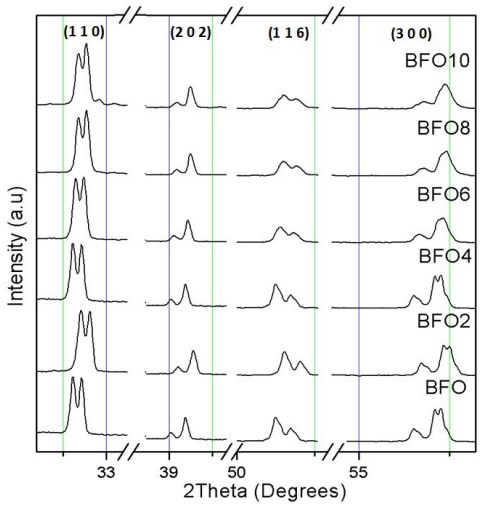

Figure 2. Enlarged XRD peaks located at 2θ values about 32, 39, 52 and 57°.

In addition, doublet peaks are characteristic of the $BFeO_3$ crystal phase. Therefore, by increasing the Sm^{3+} concentration, the peak intensity decreased. This confirms the suitable Sm^{3+} insertion in the host structure and a change in the crystal structure from a rhombohedral phase to an orthorhombic phase [9].

Fig. 2 shows enlarged XRD peaks located at 2θ values about 32, 39, 52 and 57°, matching with the (1 1 0), (2 0 2), (1 1 6) and (3 0 0) crystalline planes of the face rhombohedral structure, respectively. By increasing the Sm^{3+} concentration, the XRD peaks were shifted toward higher 2θ angles, which indicate that the unit cell was contracted. This behaviour is attributable to the smaller ionic radius of Sm^{3+} (r = 1.08 Å) regarding Bi^{3+} (r = 1.40 Å) [10].

Fig. 3 shows the refined XRD patterns for BFO10 sample. x symbols identify the experimental diffractogram, bars are the Bragg positions of identified crystal phases; green, red and blue lines are the calculated pattern, experimental difference and background, respectively. The increase in the Sm^{3+} concentration led to a contraction of the lattice parameters (Table 1), which is consistent with the shift of the XRD peaks and confirms the suitable Sm^{3+} insertion in the host structure. On the other hand, the residual factors are considerably low, indicating a high reliability of the data obtained.

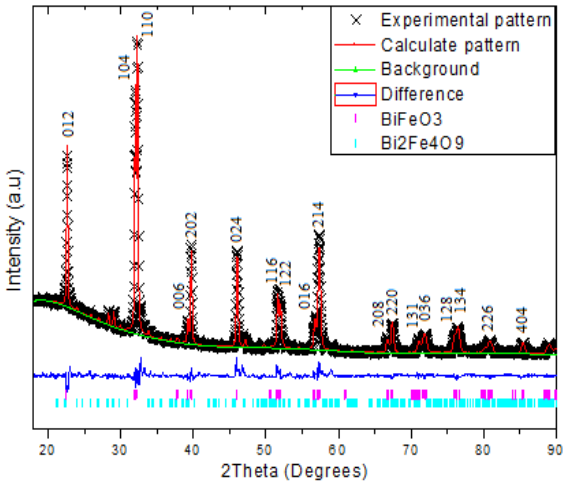

Figure 3. Refined XRD patterns for BFO10 sample.

Table 1. Lattice parameters and residual factors obtained from the Rietveld refinement.

x	Fase	a (Å)	b (Å)	c (Å)	R (%)	X²
0.00	R3c	5.5690	5.5690	13.846	0.065	2.292
0.02	R3c (88%)	5.5704	5.5704	13.845	0.095	2.548
	Pbam (12%)	7.9586	8.4516	6.001		
0.04	R3c (85%)	5.5678	5.5678	13.830	0.075	2.655
	Pbam (15%)	7.9673	8.4285	6.0209		
0.06	R3c (95%)	5.5626	5.5626	13.805	0.071	2.794
	Pbam (5%)	7.9219	8.4127	5.9866		
0.08	R3c (92%)	5.5650	5.5650	13.812	0.066	3.721
	Pbam (8%)	7.8668	8.3355	5.9180		
0.10	R3c (90%)	5.5635	5,5635	13.806	0,098	4.360
	Pbam (10%)	7.9550	8.4322	5.9913		

Fig. 4 displays the schematic crystal structure of $BiFeO_3$ unit cell. The (0 0 1) crystal orientation is equivalent to (1 1 1) of the cubic structure [11]. According to the representation, $BiFeO_3$ unit cell volume and lattice parameters are depending on the molar ratio of Sm^{3+} in the host material

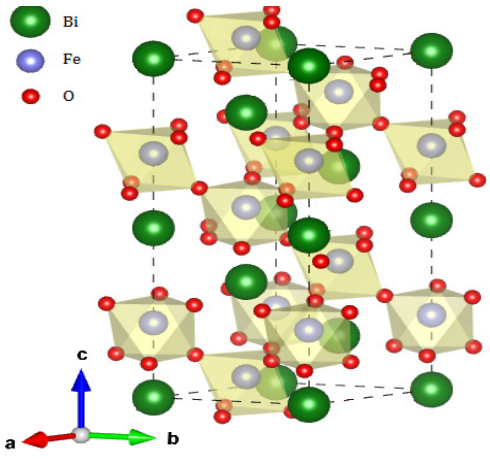

Figure 4. Schematic crystal structure of $BiFeO_3$ unit cell.

SEM images at 2000x of the BFO and BFO10 samples are shown in Figs 5a) and 5b), respectively. The SEM images show interconnected particles with well-defined edges, irregular shapes and sizes. This morphology is characteristic of $BiFeO_3$-type materials [8]. Particle size distribution was analysed using Image J software, being between 2.5 and 7.5 nm. By increasing Sm^{3+} the size of the particles decreased proportionally (see Fig. 6). This behaviour is attributable to the insertion of Sm^{3+} into the host structure and it can be correlated with the structural analysis.

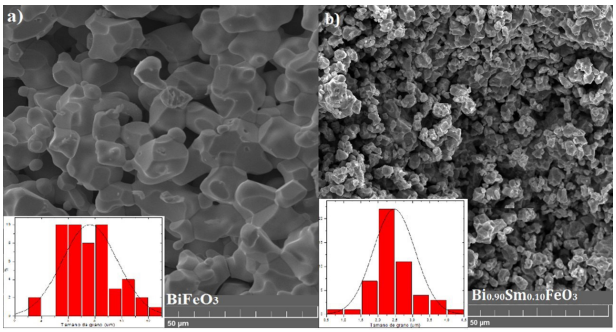

Figure 5. Images and particle size distribution of a) BFO and b) BFO10 samples.

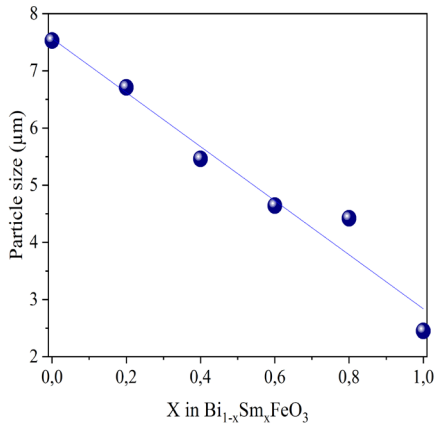

Figure 6. Particle size as a function of x in the $Bi_{1-x}Sm_xFeO_3$ system.

Fig. 7 shows the magnetic hysteresis loops at room temperature for the $Bi_{1-x}Sm_xFeO_3$ samples, with x = 0, 0.02, 0.04, 0.06, 0.08 and 0.1. Samples showed a linear increase in magnetization by increasing the applied field,

which is characteristic of the bismuth ferrite systems. Moreover, they did not exhibit a magnetic saturation, which is attributed to antiferromagnetic ordering and spin structure in the material [12].

The zoom-in section of hysteresis loops shows that the host structure ($BiFeO_3$) had a remanent magnetization ~ $2{,}02x10^{-3}$ emu/g and a coercive field ~ 178.8. This bismuth ferrite exhibits a G-type antiferromagnetic ordering, with a magnetic moment caused by a cycloid-type spatial spin of size ~ 620 Å [13-15]. On the other hand, the weak ferromagnetism at room temperature observed in the samples is mainly due to a distribution Fe^{2+} and Fe^{3+} ions to achieve compensation of oxygen vacancies and whose interaction leads to the observed spontaneous magnetization [16].

In addition, remanent magnetization and coercive field increased regarding Sm^{3+} proportion in the system (see Table 2). This increase may be explained by the collapse of the space-modulated spin structure leading to a high-range inclined antiferromagnetic order and possibly a higher degree of inclination [17].

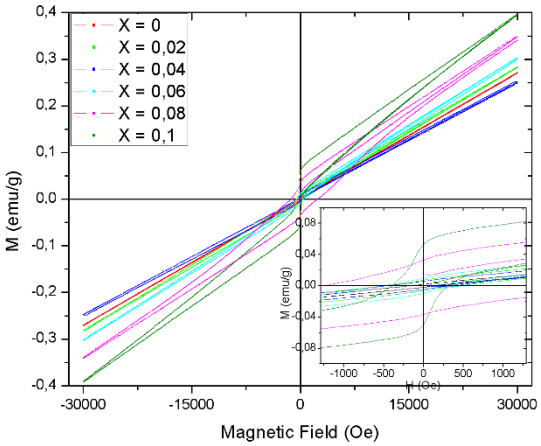

Figure 7. Magnetization as a function of magnetic field at room temperature of the $Bi_{1-x}Sm_xFeO_3$ samples.

Table 2. Remnant magnetization and cohesive field the $Bi_{1-x}Sm_xFeO_3$ samples.

Samples	M_r (emu/g)	H_c (Oe)
$BiFeO_3$	$2{,}02x10^{-3}$	178,8
$Bi_{0.98}Sm_{0.02}FeO_3$	$7{,}63x10^{-3}$	491,0
$Bi_{0.96}Sm_{0.04}FeO_3$	$6{,}22x10^{-3}$	475,7
$Bi_{0.94}Sm_{0.06}FeO_3$	$1{,}01x10^{-2}$	502,1
$Bi_{0.92}Sm_{0.08}FeO_3$	$3{,}34x10^{-2}$	1285,2
$Bi_{0.90}Sm_{0.10}FeO_3$	$5{,}33x10^{-2}$	397,3

Source: The authors

Magnetization as a function of temperature is shown in Fig. 8. Samples exhibited a PM-AFM transition characteristic of bismuth ferrite systems, which is observable at about 260 K and agree with that reported by other authors [18-20]. This behaviour is due to the effects of domain wall fixation by the random distribution of oxygen vacancies.

Magnetization at temperatures below 260 K is characteristic of AFM materials. All of the samples exhibited the AFM behaviour. However, BFO8 and BFO10 samples showed a progressive increase in magnetization by increasing the temperature. This can be attributed to the size particle reduction, leading to favouring the uncompensated antiferromagnetic spins in the material surface [8].

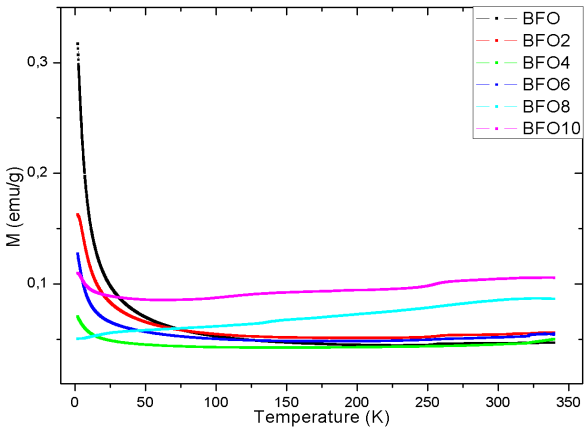

Figure 8. Magnetization as a function of temperature from 2 to 340 K for the $Bi_{1-x}Sm_xFeO_3$ system under 5000 Oe magnetic field.

4. CONCLUSIONS

Samarium-doped bismuth ferrites were successfully synthesized by the solid-state reaction method, with the higher obtention of the rhombohedral structure phase than those reported in the literature. The Rietveld refinement results confirmed the suitable insertion of the samarium in the host structure, which generated a favourable modification of the structural, morphological and magnetic properties. The morphological results showed a reduction of the particle size attributed to the difference in ionic radius that led to different nucleation phenomena. The magnetization results showed the typical ferromagnetic behaviour in the samples obtained, and the Sm^{3+} insertion generated an increase in the remanent magnetization and coercive field of the materials.

REFERENCES

[1] K. S. Nalwa & A. Garg, "Phase evolution, magnetic and electrical properties in Sm-doped bismuth ferrite". *Journal of Applied Physics,* 2008, vol. 103(4), pp. 044101. https://doi.org/10.1063/1.2838483

[2] P. Uniyal, K. L. Yadav, "Pr doped bismuth ferrite ceramics with enhanced multiferroic properties". *Journal of Physics: Condensed Matter*, 2009, vol. 21 (40), pp. 405901. https://doi.org/10.1088/0953-8984/21/40/405901

[3] P. C. Sati, P. C. Sati, M. Arora, S. Chauhan, M. Kumar, S. Chhoker, "Structural, magnetic, vibrational and impedance properties of Pr and Ti codoped BiFeO3 multiferroic ceramics". *Ceramics International*, vol. 40(6), pp. 7805-7816, 2014. https://doi.org/10.1016/j.ceramint.2013.12.124

[4] J. M. Hu, L. Q. Chen, C. W. Nan, "Multiferroic heterostructures integrating ferroelectric and magnetic materials". *Advanced materials*, vol. 28(1), pp, 15-39, 2016. https://doi.org/10.1002/adma.201502824

[5] B. H. Toby & R. B. Von Dreele, "GSAS-II: the genesis of a modern open-source all-purpose crystallography software package". *Journal of Applied Crystallography,* 2013, vol. 46, no 2, pp. 544-549. https://doi.org/10.1107/S0021889813003531

[6] W. Kraus & G. Nolze, "POWDER CELL–a program for the representation and manipulation of crystal structures and calculation of the resulting X-ray powder patterns". *Journal of applied Crystallography*, 1996, vol. 29, no 3, pp. 301-303. https://doi.org/10.1107/S0021889895014920

[7] K. Momma & F. Izumi, "VESTA 3 for three-dimensional visualization of crystal, volumetric and morphology data". *Journal of applied crystallography,* 2011, vol. 44, no 6, pp. 1272-1276. https://doi.org/10.1107/S0021889811038970

[8] A. M. Morales-Rivera, I. F. Betancourt-Montañez, S. A. Martínez-Ovalle, Ó. H. Pardo-Cuervo, J. A. Mejía-Gómez, S. Segura-Peña, C. A. Parra-Vargas, "Structural and magnetic properties of the Bi1-xLuxFeO3 (x= 0.00, 0.02 and 0.04) system". Dyna, 2020, vol. 87, no 215, pp. 84-89. https://doi.org/10.15446/dyna.v87n215.83538

[9] J. Bielecki, P. Svedlindh, D. T. Tibebu, S. Cai, S. G. Eriksson, L. Börjesson, C. S. Knee, "Structural and magnetic properties of isovalently substituted multiferroic BiFeO3: insights from Raman spectroscopy". *Physical Review* B, 2012, vol. 86, no 18, pp. 184422. DOI: https://doi.org/10.1103/PhysRevB.86.184422

[10] N. Zhang, J. Q. Ding, Y. P. Wang, X. N. Liu, Y. Q. Li, M. F. Liu, Z. M. Fu, Y. W. Yang, J. Su, G. L. Song, F. Yang, Y. Y. Guo and J-M Liu, "Enhanced high temperature ferromagnetism in Bi1–xRxFeO3 (R= Dy, Y) compounds". *Journal of Physics: Condensed Matter*, 2021, vol. 33, no 13, pp. 135803. https://doi.org/10.1088/1361-648X/abdb10

[11] J. G. Park, M. D. Le, J. Jeong and S. Lee, "Structure and spin dynamics of multiferroic BiFeO3". *Journal of Physics: Condensed Matter*, 2014, vol. 26, no 43, pp. 433202. https://doi.org/10.1088/0953-8984/26/43/433202

[12] R. Köferstein, "Synthesis, phase evolution and properties of phase-pure nanocrystalline BiFeO3 prepared by a starch-based combustion method". *Journal of alloys and compounds*, 2014, vol. 590, pp. 324-330. https://doi.org/10.1016/j.jallcom.2013.12.120

[13] T. J. Park, G. C. Papaefthymiou, A. J. Viescas, A. R. Moodenbaugh and S. S. Wong, "Size-dependent magnetic properties of single-crystalline multiferroic BiFeO3 nanoparticles". *Nano letters*, 2007, vol. 7, no 3, pp. 766-772. https://doi.org/10.1021/nl063039w

[14] E. R. Ochoa-Burgos, C. A. Parra-Vargas, J. A. Mejía-Gómez & E. de Grave, "Study of the structural and magnetic properties of the system Bi1-xYxFeO3 x= 0 and 0.07 using Mössbauer spectroscopy". *Dyna*, 2018, vol. 85, no 207, pp. 22-28. https://doi.org/10.15446/dyna.v85n207.68421

[15] D. V. Karpinsky, A. Pakalniškis, G. Niaura, D. V. Zhaludkevich, A. L. Zhaludkevich, S. I. Latushka, A. Kareiva, "Evolution of the crystal structure and magnetic properties of Sm-doped BiFeO3 ceramics across the phase boundary region". *Ceramics International*, 2021, vol. 47, no 4, pp. 5399-5406. https://doi.org/10.1016/j.ceramint.2020.10.120

[16] C. A. Narváez, C. F. Vilaquirán-Raigoza, A. P. González-Nieva, "Modificación de las propiedades estructurales, eléctricas y magnéticas del BiFeO3 por la incorporación de Ba y Nb". *Química Nova*, 2017, vol. 40, no.2, p. 182-191. http://dx.doi.org/10.21577/0100-4042.20160185

[17] D. Maurya, H. Thota, A. Garg, B. Pandey, P. Chand and H. C. Verma, "Magnetic studies of multiferroic Bi1−xSmxFeO3 ceramics synthesized by mechanical activation assisted processes". *Journal of Physics: Condensed Matter*, 2008, vol. 21, no 2, pp. 026007. https://doi.org/10.1088/0953-8984/21/2/026007

[18] M. A. Basith, A. Billah, M. A. Jalil, N. Yesmin, M. A. Sakib, E. K. Ashik, B. Ahmmad, "The 10% Gd and Ti co-doped BiFeO3: a promising multiferroic material". *Journal of Alloys and Compounds*, 2017, vol. 694, pp. 792-799. https://doi.org/10.1016/j.jallcom.2016.10.018

[19] T. Durga Rao & S. Asthana, "Evidence of improved ferroelectric phase stabilization in Nd and Sc co-substituted BiFeO3". *Journal of Applied Physics*, 2014, vol. 116, no 16, p. 164102. https://doi.org/10.1063/1.4898805

[20] L. M. Ramirez-Guzmán, A. F. Cruz-Pacheco, J. A. Gómez-Cuaspud & C. A. Parra-Vargas, "Structural and magnetic properties of gadolinium modified BiFeO3". *Materials Science Poland*, 2020, vol. 38. https://doi.org/10.2478/msp-2020-0075